

Status of the global electroweak fit of the Standard Model

Andreas Hoecker^{*†}

CERN CH-1211, Geneva 23, Switzerland

E-mail: andreas.hoecker@cern.ch

Results from the global Standard Model fit to electroweak precision data, including newest Tevatron measurements, are reviewed and discussed. The complete fit using also the constraints from the direct Higgs boson searches yields an upper limit on the Higgs mass of 153 GeV at 95% CL. The top mass is indirectly determined to be $177.2^{+10.5}_{-7.8}$ GeV and $179.5^{+8.8}_{-5.2}$ GeV for fits including or not the constraints from the direct Higgs searches, respectively. Using the 3NLO perturbative prediction of the massless QCD Adler function, the strong coupling constant at the Z-mass scale is determined to be $\alpha_s(M_Z^2) = 0.1193 \pm 0.0028 \pm 0.0001$, which is in excellent agreement with the 3NLO result from hadronic τ decays. The perspectives of the electroweak fit for forthcoming and proposed future collider projects are discussed. The available constraints on the Higgs mass are convolved with the high-scale behaviour of the Higgs quartic coupling to derive likelihoods for the survival of the Standard Model versus its cut-off scale evolved up to the Planck mass.

*The 2009 Europhysics Conference on High Energy Physics
Krakow, Poland
July 16 – 22, 2009*

^{*}Speaker.

[†]For the Gfitter Group: M. Baak (CERN), M. Goebel (DESY and U. Hamburg), H. Flücher (CERN), J. Haller (U. Hamburg), A. Hoecker (CERN), D. Ludwig (DESY and U. Hamburg), K. Mönig (DESY), M. Schott (CERN) and J. Stelzer (DESY).

1. Introduction

Precision measurements allow us, by exploiting contributions from quantum loops, to probe physics at much higher energy scales than the masses of the particles directly involved in experimental reactions. These tests do not only require accurate and well understood experimental data but also theoretical predictions with controlled uncertainties that match the experimental precision. Prominent examples are the LEP precision measurements, which were used in conjunction with the Standard Model (SM) to predict via multidimensional parameter fits the mass of the top quark [1], prior to its observation at the Tevatron [2].¹ Later, when combined with the measured top mass, the same approach led to the prediction of a light Higgs boson [3].

Several theoretical libraries within and beyond the SM have been developed in the past, which allowed to constrain the unbound parameters of the SM [4,5]. However, most of these programmes are relatively old, were implemented in outdated programming languages, and are difficult to maintain in line with the theoretical and experimental progress. It is unsatisfactory to rely on them during the forthcoming era of the Large Hadron Collider (LHC) and the preparations for future linear collider projects. Improved measurements of important input observables are expected and new observables from discoveries may augment the available constraints. None of the previous programmes are modular enough to easily allow the theoretical predictions to be extended to models beyond the SM, and they are usually tied to a particular minimisation package.

These considerations led to the development of the generic fitting package *Gfitter* [6], designed to provide a framework for model testing in high-energy physics. *Gfitter* is implemented in C++ and relies on ROOT [7] functionality, XML and python. Theoretical models are inserted as plugin packages. Tools for the handling of the data, the fitting, and statistical analyses such as pseudo Monte Carlo sampling are provided by a core package, where theoretical errors, correlations, and inter-parameter dependencies are consistently dealt with. The use of dynamic parameter caching avoids the recalculation of unchanged results between fit steps, and thus significantly reduces the amount of computing time required for a fit.

These proceedings review the current status of the global electroweak fit and discuss the perspectives of the fit for forthcoming and future collider projects. Following Ref. [27] we also review the evolution properties of the quartic coupling in the SM Higgs potential to high scales, and combine them with the available constraints on the Higgs boson mass. More detailed information on the latter topic has been presented at this conference [9]. Reference [8] reviews the status of beyond SM constraints with *Gfitter*.

2. The global electroweak fit of the Standard Model

The SM predictions for the electroweak precision observables measured by the LEP, SLC, and Tevatron experiments are fully implemented in *Gfitter*. State-of-the-art calculations have been

¹The importance of radiative corrections at the EW scale can be illustrated by comparing the tree-level EW unification prediction of the W mass, $M_W^{(0)2} = (M_Z^2/2)(1 + \sqrt{1 - \sqrt{8}\pi\alpha/G_F M_Z^2}) = (79.964 \pm 0.005)$ GeV, with the world average measurement, $M_W = (80.399 \pm 0.023)$ GeV, exhibiting a 18.5σ discrepancy due to a 0.5% contribution from loop effects. The dominant one-loop diagrams are bosonic and fermionic vacuum polarisation and self energies, as well as top- W corrections to the $Z \rightarrow b\bar{b}$ vertex. Their dependence on the top and Higgs boson mass parameters are respectively quadratic and logarithmic.

used, and the results were thoroughly cross-checked against ZFITTER [4]. For the W mass and the effective weak mixing angle, which exhibit the strongest constraints on the Higgs mass, the full second order corrections are available [10]. Furthermore, corrections of order $\mathcal{O}(\alpha\alpha_s^2)$ and leading three-loop corrections in an expansion of the top-mass-squared (m_t^2) are included. The full three-loop corrections are known in the large M_H limit, however they turn out to be negligibly small [11]. The partial and total widths of the Z are known to leading order, while for the second order only the leading m_t^2 corrections are available [12]. Among the new developments included in the SM library is the fourth-order (3NLO) perturbative calculation of the massless QCD Adler function [13], contributing to the vector and axial-vector radiator functions in the prediction of the Z hadronic width (and other observables). It allows to fit the strong coupling constant with unique theoretical accuracy.

Among the experimental precision data used are the Z mass, measured with relative precisions of $2 \cdot 10^{-5}$ at LEP, and the hadronic pole cross section and leptonic decay width ratio of the Z , both known to $9 \cdot 10^{-4}$ relative precision. The effective weak mixing angle $\sin^2\theta_{\text{eff}}^\ell$ is known to a relative precision of $7 \cdot 10^{-4}$ from the measurements of the left-right and forward-backward asymmetries for universal leptons and heavy quarks by the LEP and SLD experiments. The W mass has been measured at LEP and the Tevatron to an overall relative precision of $3 \cdot 10^{-4}$. We include the new preliminary result reported by D0 [14] and combine it with the previous world average to the preliminary average 80.399 ± 0.023 , taking into account correlations between systematic errors.² The top mass has been measured to $7 \cdot 10^{-3}$ relative precision at the Tevatron. We use the newest average $m_t = (173.1 \pm 0.6 \pm 1.1)$ GeV [16], where the first error is statistical and the second systematic. Also required is the knowledge of the electromagnetic coupling strengths at the M_Z scale, which is modified with respect to the Thomson scattering limit due to energy-dependent photon vacuum polarisation contributions. It is known to a relative precision of $8 \cdot 10^{-3}$, dominated by the uncertainty in the hadronic contribution from the five lightest quarks, $\Delta\alpha_{\text{had}}^{(5)}(M_Z^2)$. Finally, the Fermi constant, parametrising the weak coupling strength, is known to $4 \cdot 10^{-5}$ relative precision.

We also fold into the fit the information from the direct Higgs boson searches at LEP [17] and Tevatron, where for the latter experiments the latest combination is used [18], including a rising number of search channels with up to 4.2 fb^{-1} integrated luminosity. All experiments use as test statistics the negative logarithm of a likelihood ratio, $-2\ln Q$, of the SM Higgs signal plus background (s + b) to the background-only (b) hypotheses. This choice ensures $-2\ln Q = 0$ when there is no experimental sensitivity to a Higgs signal. The corresponding one-sided confidence levels $\text{CL}_{\text{s+b}}$ and CL_{b} describe the probabilities of upward fluctuations of the test statistics in presence and absence of a signal, respectively ($1 - \text{CL}_{\text{b}}$ is thus the probability of a false discovery). They are derived using pseudo Monte Carlo (MC) experiments. Using the modified quantity $\text{CL}_{\text{s}} = \text{CL}_{\text{s+b}}/\text{CL}_{\text{b}}$ the combination of LEP searches [17] has set the lower limit $M_H > 114.4$ GeV at 95% CL, and the Tevatron experiments recently reported the exclusion of the range $160 < M_H < 170$ GeV at and above 95% CL [18]. Because in the EW fit we are interested in the *deviation* of a measurement from the SM hypothesis, we transform $\text{CL}_{\text{s+b}}$ into a two-sided confidence level given by $2\text{CL}_{\text{s+b}}$ for $\text{CL}_{\text{s+b}} \leq 0.5$ and $2(1 - \text{CL}_{\text{s+b}})$ otherwise. The contribution to the χ^2 estimator of the fit is then obtained via $\delta\chi^2 = 2 \cdot [\text{Erf}^{-1}(1 - \text{CL}_{\text{s+b}}^{2\text{-sided}})]^2$. The alternative (Bayesian) direct use of the

²Our M_W average agrees with the recently published official Tevatron value [15].

test statistics $-2\ln Q$ in the fit leads to a similar behaviour as $\delta\chi^2$ with however an overall shift of approximately one unit due to a deeper minimum, thus resulting in a slightly stronger constraint on M_H (cf. lower plot in Fig. 1 with the $-2\ln Q$ curve drawn dashed).

Global fits are performed in two versions: the *standard* (“blue-band”) fit makes use of all the available information except for results from direct Higgs boson searches; the *complete fit* uses also the constraints from the Higgs searches at LEP and Tevatron. The free fit parameters are M_Z , M_H , m_t , m_c , m_b , $\Delta\alpha_{\text{had}}^{(5)}(M_Z^2)$, and $\alpha_s(M_Z^2)$, where only the latter parameter is fully unconstrained (apart from M_H in the standard fit). Theoretical uncertainties due to missing higher order perturbative corrections in the predictions of M_W and $\sin^2\theta_{\text{eff}}^f$ and in the electroweak form factors ρ_Z^f and κ_Z^f are included in the fit by means of scale parameters according to the *Rfit* prescription [19]. The relevant input parameters and fit results are summarised in Table 1, and discussed below.

- The minimum χ^2 of the standard (complete) fit amounts to 16.4 (17.9) for 13 (14) degrees of freedom. The corresponding p-value for wrongly rejecting the SM from the result of the complete fit, obtained with pseudo-MC samples, is $0.20 \pm 0.01_{-0.02}$, where the first error is statistical and the second is the difference obtained when fixing or varying the theoretical parameters. We also notice that none of the pull values after fit convergence exceeds 3σ .
- The correlation coefficients between M_H on one hand, and m_t , $\Delta\alpha_{\text{had}}^{(5)}(M_Z^2)$, and M_W on the other are 0.31, -0.40 , and -0.54 , respectively. They are small for all other floating fit parameters. In particular, the small correlation with $\alpha_s(M_Z^2)$ allows for an independent determination of this quantity, not affected by the unknown Higgs properties.
- Some input observables, such as M_Z , are much better known than it is required for the fit (the experimental precision exceeds the fit sensitivity by a factor of 10), so that they could have been fixed in the fit without significant change in the results. Others, such as Γ_W , are not well enough known to impact the fit (the fit sensitivity exceeds the measurement precision by a factor of almost 50). And finally, observables such as M_W and m_t are driving the fit precision. Here is where the experimental effort must concentrate on.
- We find $M_H = 83_{-23}^{+30}$ GeV (standard fit) and $M_H = 116_{-1.3}^{+16}$ GeV (complete fit) with the 2σ intervals $[42, 158]$ GeV and $[114, 153]$ GeV, respectively (cf. top and middle plots in Fig. 1). At 3σ the complete fit still allows Higgs masses between 180 and 227 GeV, which the Tevatron experiments should have the sensitivity to exclude soon. Figure 2 shows the 68%, 95% and 99% CL contours for the variable pairs m_t vs. M_H (top plot) and $\Delta\alpha_{\text{had}}^{(5)}(M_Z^2)$ vs. M_H (middle), exhibiting the largest correlations in the fits. The contours are derived from the $\Delta\chi^2$ values found in the profile scans using $\text{Prob}(\Delta\chi^2, 2)$. Three sets of fits are shown in these plots: the largest/blue (narrower/purple) allowed regions are derived from the standard fit excluding (including) the measured values (indicated by shaded/light green horizontal bands) for respectively m_t and $\Delta\alpha_{\text{had}}^{(5)}(M_Z^2)$ in the fits. The correlations seen in these plots are approximately linear for $\ln M_H$. The third set of fits, providing the narrowest constraints, uses the complete fit, *i.e.*, including in addition to all available measurements the direct Higgs searches.

Parameter	Input value	Free in fit	Results from global EW fits:		<i>Complete fit w/o exp. input in line</i>
			<i>Standard fit</i>	<i>Complete fit</i>	
M_Z [GeV]	91.1875 ± 0.0021	yes	91.1874 ± 0.0021	91.1876 ± 0.0021	$91.1974^{+0.0191}_{-0.0159}$
Γ_Z [GeV]	2.4952 ± 0.0023	–	2.4960 ± 0.0015	2.4956 ± 0.0015	$2.4952^{+0.0017}_{-0.0016}$
σ_{had}^0 [nb]	41.540 ± 0.037	–	41.478 ± 0.014	41.478 ± 0.014	41.469 ± 0.015
R_ℓ^0	20.767 ± 0.025	–	20.742 ± 0.018	20.741 ± 0.018	20.717 ± 0.027
$A_{\text{FB}}^{0,\ell}$	0.0171 ± 0.0010	–	0.01638 ± 0.0002	0.01624 ± 0.0002	$0.01617^{+0.0002}_{-0.0001}$
$A_\ell^{(*)}$	0.1499 ± 0.0018	–	0.1478 ± 0.0010	$0.1472^{+0.0009}_{-0.0008}$	–
A_c	0.670 ± 0.027	–	$0.6682^{+0.00045}_{-0.00044}$	$0.6679^{+0.00042}_{-0.00036}$	$0.6679^{+0.00041}_{-0.00036}$
A_b	0.923 ± 0.020	–	0.93469 ± 0.00010	$0.93463^{+0.00007}_{-0.00008}$	$0.93463^{+0.00007}_{-0.00008}$
$A_{\text{FB}}^{0,c}$	0.0707 ± 0.0035	–	$0.0741^{+0.0006}_{-0.0005}$	0.0737 ± 0.0005	0.0737 ± 0.0005
$A_{\text{FB}}^{0,b}$	0.0992 ± 0.0016	–	0.1036 ± 0.0007	$0.1032^{+0.0007}_{-0.0006}$	$0.1037^{+0.0004}_{-0.0005}$
R_c^0	0.1721 ± 0.0030	–	0.17225 ± 0.00006	0.17225 ± 0.00006	0.17225 ± 0.00006
R_b^0	0.21629 ± 0.00066	–	0.21578 ± 0.00005	0.21577 ± 0.00005	0.21577 ± 0.00005
$\sin^2 \theta_{\text{eff}}^\ell(Q_{\text{FB}})$	0.2324 ± 0.0012	–	0.23142 ± 0.00013	$0.23151^{+0.00010}_{-0.00012}$	$0.23149^{+0.00013}_{-0.00010}$
M_H [GeV] ^(o)	Likelihood ratios	yes	$83^{+30[+75]}_{-23[-41]}$	$116^{+15.6[+36.5]}_{-1.3[-2.2]}$	$83^{+30[+75]}_{-23[-41]}$
M_W [GeV]	80.399 ± 0.023	–	$80.384^{+0.014}_{-0.015}$	$80.371^{+0.008}_{-0.011}$	$80.361^{+0.013}_{-0.012}$
Γ_W [GeV]	2.098 ± 0.048	–	$2.092^{+0.001}_{-0.002}$	2.092 ± 0.001	2.092 ± 0.001
\bar{m}_c [GeV]	1.25 ± 0.09	yes	1.25 ± 0.09	1.25 ± 0.09	–
\bar{m}_b [GeV]	4.20 ± 0.07	yes	4.20 ± 0.07	4.20 ± 0.07	–
m_t [GeV]	173.1 ± 1.3	yes	173.2 ± 1.2	173.6 ± 1.2	$179.5^{+8.8}_{-5.2}$
$\Delta\alpha_{\text{had}}^{(5)}(M_Z^2)$ ^(†Δ)	2767 ± 22	yes	2772 ± 22	2764^{+22}_{-21}	2733^{+57}_{-63}
$\alpha_s(M_Z^2)$	–	yes	$0.1192^{+0.0028}_{-0.0027}$	0.1193 ± 0.0028	0.1193 ± 0.0028
$\delta_{\text{th}} M_W$ [MeV]	$[-4, 4]_{\text{theo}}$	yes	4	4	–
$\delta_{\text{th}} \sin^2 \theta_{\text{eff}}^\ell$ ^(†)	$[-4.7, 4.7]_{\text{theo}}$	yes	4.7	0.8	–
$\delta_{\text{th}} \rho_Z^f$ ^(†)	$[-2, 2]_{\text{theo}}$	yes	2	2	–
$\delta_{\text{th}} \kappa_Z^f$ ^(†)	$[-2, 2]_{\text{theo}}$	yes	2	2	–

(*) Average of LEP and SLD. (o) In brackets the 2σ . (†) In units of 10^{-5} . (Δ) Rescaled due to α_s dependency.

Table 1: Input values and fit results for parameters of the global electroweak fit. The first and second columns list respectively the observables/parameters used in the fit, and their experimental values or phenomenological estimates (see text for references). The subscript “theo” labels theoretical error ranges. The third column indicates whether a parameter is floating in the fit. The fourth (fifth) column quotes the results of the *standard (complete) fit* not including (including) the constraints from the direct Higgs searches at LEP and Tevatron in the fit. In case of floating parameters the fit results are directly given, while for observables, the central values and errors are obtained by individual profile likelihood scans. The errors are derived from the $\Delta\chi^2$ profile using a Gaussian approximation. The last column gives the fit results for each parameter without using the corresponding experimental constraint in the fit (indirect determination).

- There is a well-known tension between the M_H results for the most sensitive observables. For $A_\ell(\text{LEP})$, $A_\ell(\text{SLD})$, $A_{\text{FB}}^{0,b}$ and M_W we find respectively $M_H = 104_{-64}^{+148}$, 26_{-16}^{+25} , 371_{-166}^{+295} , and 42_{-22}^{+56} (all values in GeV). Evaluating with pseudo-MC experiments, taking into account all known correlations, the probability to observe a value of $\Delta\chi^2 = 8.0$ when removing the least compatible of the four measurements from the fit, gives 1.4% corresponding to an equivalent of 2.5σ .
- Without using the direct m_t measurement, the standard and complete fits determine the top mass to be $177.2_{-7.8}^{+10.5}$ GeV and $179.5_{-5.2}^{+8.8}$ GeV, respectively, where the latter result is 1.2σ away from the experimental value requiring a smaller M_H , which is excluded by LEP, or a smaller M_W value (see next bullet). It is noticeable that the standard fit without using the measured top-mass gives $M_H = 116_{-61}^{+184}$ GeV with a central value equal to the complete fit (though with largely inflated errors).
- One can also indirectly determine M_W from the fit without using the input from the direct measurements. The results from the standard and complete fits read $M_W = 80.374_{-0.038}^{+0.019}$ GeV and $80.361_{-0.012}^{+0.013}$ GeV, respectively, requiring a smaller value when including the M_H constraints. The bottom plot in Fig. 2 compares the direct measurements of m_t and M_W , shown by the shaded/green 1σ bands, with the 68%, 95% and 99% CL constraints obtained with three fit scenarios. The largest/blue (narrowest/green) allowed regions are the result of the standard fit (complete fit) excluding (including) the measured values of M_W and m_t . The results of the complete fit excluding the measured values are illustrated by the narrower/yellow allowed region. The allowed regions of the indirect determination is significantly reduced with the insertion of the direct Higgs searches.
- Among the most important outcomes of the fit is the 3NLO [13] precision determination of $\alpha_s(M_Z^2)$ obtained mainly by the parameter R_ℓ^0 . One finds $\alpha_s(M_Z^2) = 0.1193 \pm 0.0028 \pm 0.0001$, where the first error is experimental and the second due to the truncation of the perturbative series. It includes variations of the renormalisation scale between $0.6M_Z < \mu < 1.3M_Z$ [20], of massless terms of order $\alpha_s^5(M_Z)$ and higher, and of quadratic massive terms of order and beyond $\alpha_s^4(M_Z)$. The result is in excellent agreement with the precise 3NLO determination from hadronic τ decays, which, evolved to the Z -mass scale, reads $\alpha_s(M_Z^2) = 0.1212 \pm 0.0005 \pm 0.0009$ [20], dominated by theoretical uncertainties.³ These two measurements represent the best current test of the asymptotic freedom property of QCD (*cf.* Fig. 3).

3. Future prospects

Several improved measurements are expected from the LHC [25]. The Higgs boson should

³Only partly contained in the theoretical error are systematic differences arising from the computation of the contour integral, denoted as fixed-order perturbation theory (FOPT) and contour-improved fixed-order perturbation theory (CIPT), respectively. The value cited here uses CIPT. The differences between FOPT and CIPT are discussed in Refs. [13,20–23].

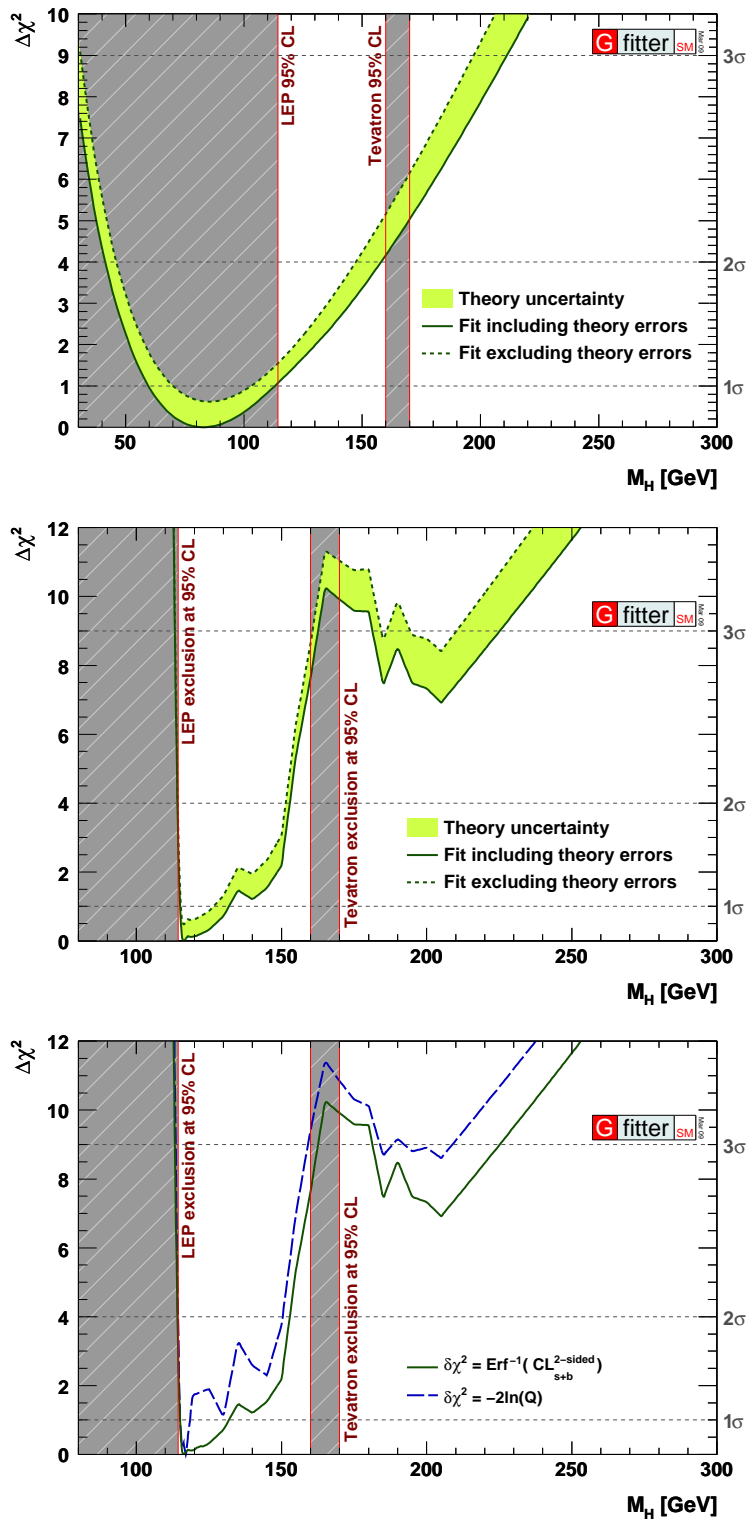


Figure 1: $\Delta\chi^2$ as a function of M_H for the standard fit (top) and the complete fit (middle). The solid (dashed) lines give the results when including (ignoring) theoretical errors. The bottom plot shows the results from the complete fit with the two-sided CL_{s+b} method (solid line, same as middle plot) and the direct use of $\Delta\chi^2 = -2\ln Q$ as estimator (dashed). The minimum $\Delta\chi^2$ being deeper for the latter method, the overall curve is shifted.

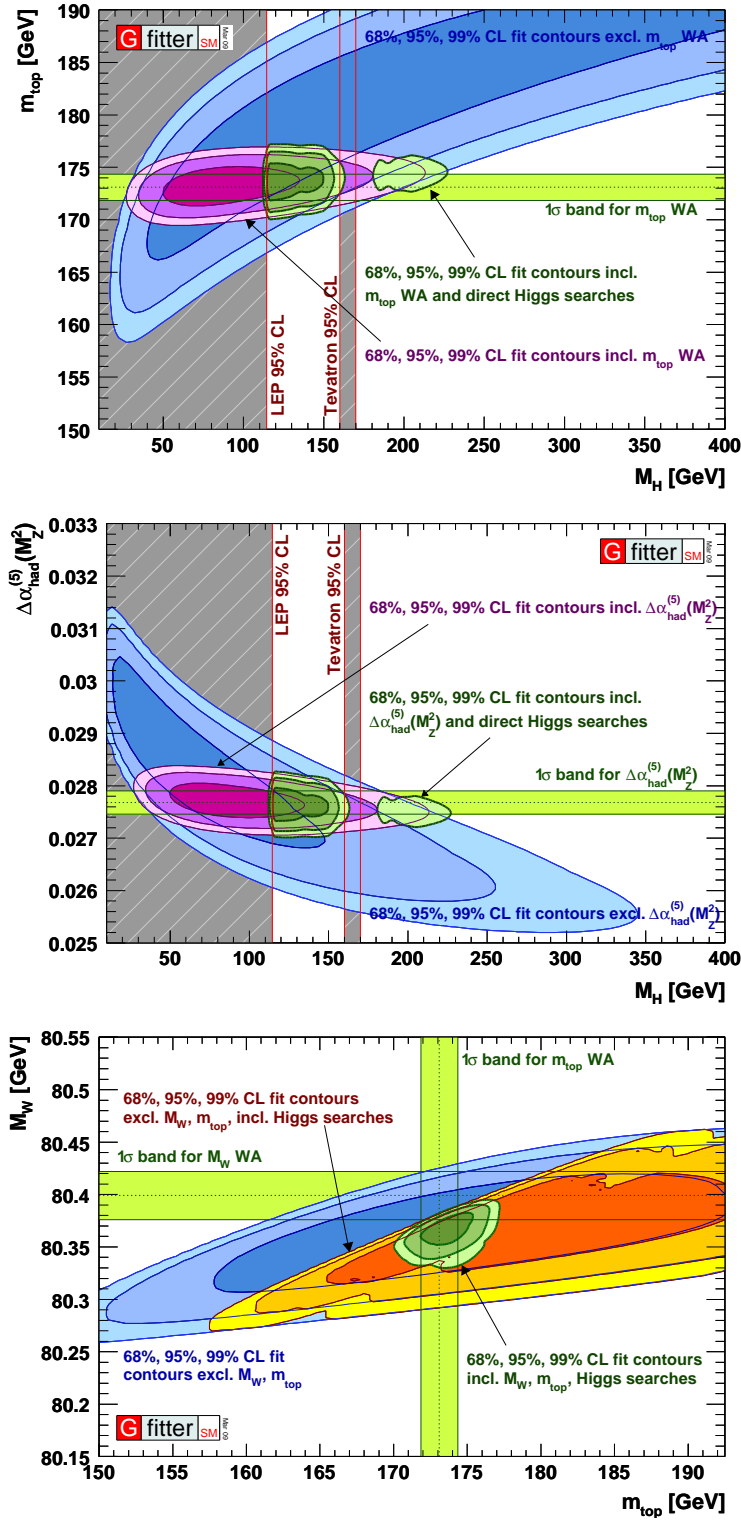


Figure 2: Contours of 68%, 95% and 99% CL obtained from scans of fits with fixed variable pairs m_t vs. M_H (top), $\Delta\alpha_{\text{had}}^{(5)}(M_Z^2)$ vs. M_H (middle), and M_W vs. m_t (bottom). The conditions of the various fits shown are indicated on the plots. The horizontal bands depict the 1σ regions of the current world average measurements (or phenomenological determination in case of $\Delta\alpha_{\text{had}}^{(5)}(M_Z^2)$).

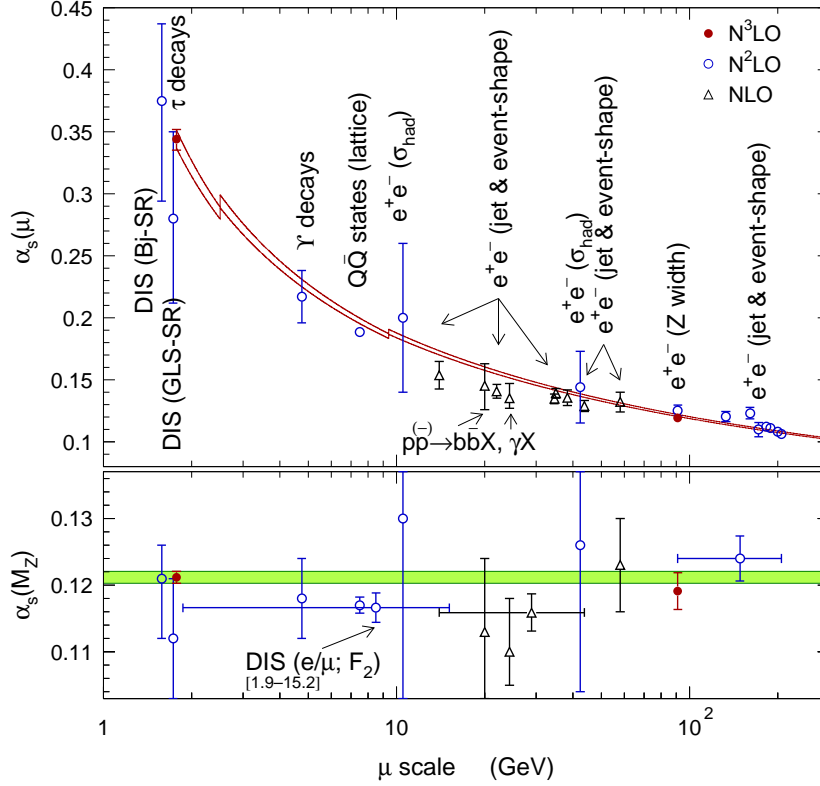


Figure 3: Evolution of $\alpha_s(m_\tau^2)$ to higher scales μ using the four-loop RGE and the three-loop matching conditions applied at the heavy quark-pair thresholds (hence the discontinuities at $2\bar{m}_c$ and $2\bar{m}_b$). The evolution is compared with measurements at different scales (from Ref. [24] and including newer measurements) covering more than two orders of magnitude. The bottom part shows the corresponding α_s values evolved to M_Z . The shaded band displays the τ decay result within errors. Only the τ and Z -scale measurements have 3NLO theoretical accuracy. The figure is taken from Ref. [20].

be discovered leaving the SM without an unmeasured parameter.⁴ The focus of the global SM fit would then move from parameter estimation to the analysis of the goodness-of-fit with the goal to uncover inconsistencies between the model and the data, indicating the presence of new physics. Because the Higgs-boson mass enters only logarithmically in the loop corrections, a precision measurement is not required for this purpose. With the LHC the uncertainty on the W -boson and the top-quark masses should shrink to 15 MeV and 1 GeV, respectively. The fit constraint on M_H for a hypothetical 120 GeV Higgs boson would improve from currently 120_{-40}^{+50} GeV to 120_{-35}^{+45} GeV (assuming unchanged theoretical errors).

At the ILC, a significant increase in the top mass precision to an error of at least 0.2 GeV from a threshold scan is expected, providing a Higgs mass constraint of 120_{-33}^{+42} GeV. If in the meantime the prediction of $\Delta\alpha_{\text{had}}^{(5)}(M_Z^2)$ has been improved to an accuracy of, say, $7 \cdot 10^{-5}$, by virtue of more accurate hadronic cross section data at low and intermediate energies, one could achieve $M_H = 120_{-31}^{+39}$ GeV.

⁴Excluding here the massive neutrino sector, requiring at least nine additional parameters, which are however irrelevant for the results discussed here.

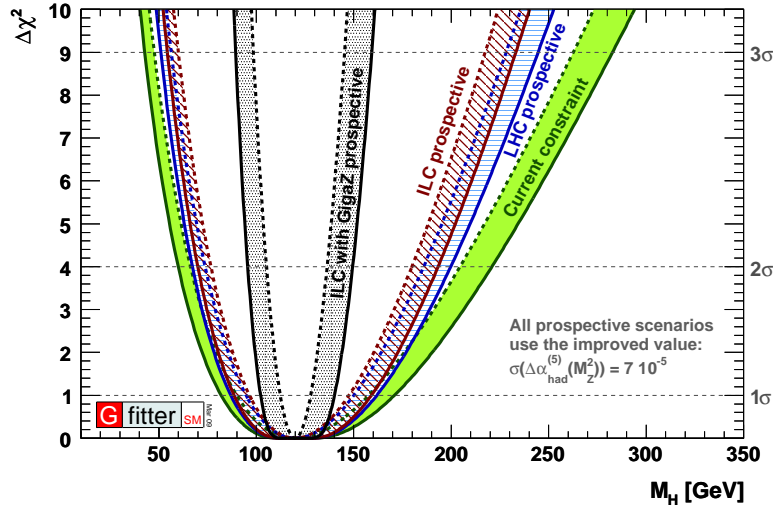


Figure 4: Constraints on M_H obtained for the four future scenarios discussed in the text. An improvement of $\sigma(\Delta\alpha_{\text{had}}^{(5)}(M_Z^2)) = 7 \cdot 10^{-5}$ is assumed for all prospective curves. The shaded bands indicate the contributions from theoretical uncertainties in the EW theory.

Running the ILC at lower energy with polarised beams (Giga-Z), the W and top masses could be determined to better than 6 MeV and 0.1 GeV, respectively. Moreover, the weak mixing angle is expected to be measured to a precision of $1.3 \cdot 10^{-5}$ [26], and R_ℓ^0 to 0.004, resulting in an unprecedented precision determination of $\alpha_s(M_Z^2)$ with an error of 0.0006, *i.e.*, a factor of 3 improvement over the current value. Owing to the small theoretical error at 3NLO such a precision could be fully exploited [13]. The improvements on the prediction of the Higgs mass are dramatic for Giga-Z where we find for a 120 GeV Higgs fit errors of about 19 GeV, assuming the improved $\Delta\alpha_{\text{had}}^{(5)}(M_Z^2)$. Such a constraint on M_H will be significantly affected by from theoretical errors (without theory errors one could constrain the Higgs mass to 8 GeV), requiring improved electroweak calculations.

The M_H scans obtained for the four scenarios, assuming the improved $\Delta\alpha_{\text{had}}^{(5)}(M_Z^2)$ precision to be applicable for all future scenarios, are shown in Fig. 4. The shaded bands indicate the effects of the current theoretical uncertainties. The theoretical errors treated with the Rfit scheme are recognised by the broad plateaus around the $\Delta\chi^2$ minimum.

In case of the discovery of a light Higgs, and a precise mass measurement (expected to be 0.1% or better for $H \rightarrow \gamma\gamma$), the W boson mass could be predicted with 13 MeV error, of which 5 MeV is (currently) theoretical. With the new machines, new precision measurements would enter the fit, namely the two-fermion cross section at higher energies and the electroweak triple gauge boson couplings, which are sensitive to models beyond the SM. Most importantly however, both machines are directly sensitive to new phenomena and thus either provide additional constraints on fits of new physics models or, if the searches are successful, may completely alter our picture of the terascale physics. The SM will then require extensions, the new parameters of which must be determined by a global fit, whose goodness must also be probed.

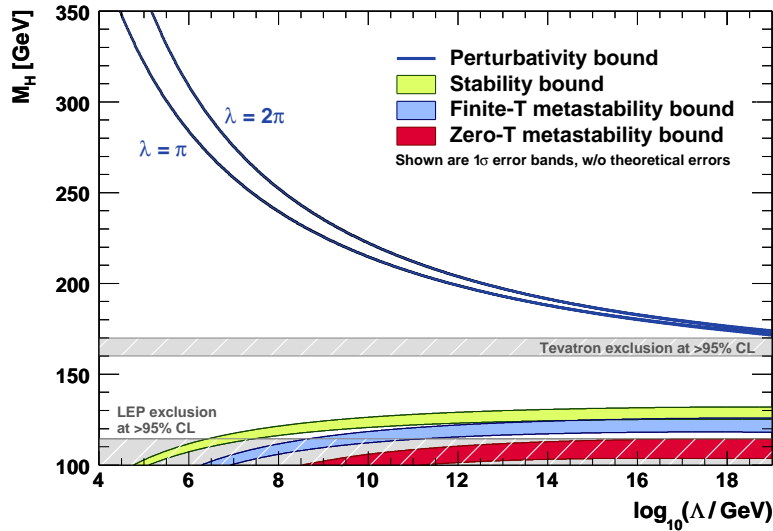


Figure 5: The scale Λ at which the two-loop RGEs drive the quartic SM Higgs coupling non-perturbative, and the scale Λ at which the RGEs create an instability in the electroweak vacuum ($\lambda < 0$). The width of the bands indicates the errors induced by the uncertainties in the top mass and in α_s (added quadratically). The perturbativity upper bound (sometimes referred to as “triviality” bound) is given for $\lambda = \pi$ (lower bold line) and $\lambda = 2\pi$ (upper bold line). Their difference indicates the size of the theoretical uncertainty in this bound. The absolute vacuum stability bound is displayed by the light shaded (green) band, while the less restrictive finite-temperature and zero-temperature metastability bounds are medium (blue) and dark shaded (red), respectively. The theoretical uncertainties in these bounds have been ignored in the plot for the purpose of clarity. The grey hatched areas indicate the LEP [17] and Tevatron [18] exclusion domains. The figure is taken from Ref. [27].

4. The fate of the Standard Model

The Higgs sector of the SM must steer a narrow course between two problematic situations if it is to survive up to the reduced Planck scale $M_P \sim 2 \cdot 10^{18}$ GeV. If M_H is large enough, the renormalisation-group equations (RGEs) of the SM drive the Higgs self-coupling into the non-perturbative regime at some scale $\Lambda < M_P$, entailing either new non-perturbative physics at a scale $\sim \Lambda$, or new physics at some scale $< \Lambda$ that prevents the Higgs self-coupling from becoming non-perturbative. This is shown as the upper pair of bold (blue) lines in Fig. 5 [27]. On the other hand, if M_H is small enough, the RGEs drive the Higgs self-coupling to a negative value at some Higgs field value $\Lambda < M_P$, in which case the electroweak vacuum is only a local minimum and there is a new, deep and potentially dangerous minimum at scales $> \Lambda$. The electroweak vacuum can become unstable against collapse because of zero-temperature or thermal tunneling during the evolution of the universe into that deeper new vacuum with Higgs vacuum expectation value $> \Lambda$, unless there is new physics at some scale $< \Lambda$ that prevents the appearance of that vacuum. This lower bound is shown with its uncertainties by the light shaded (green) band in Fig. 5. Below this stability bound, there is a metastability region, where the total quantum tunneling probability throughout the period of the history of the Universe is small enough so that the electroweak vacuum has a lifetime longer than the age of the Universe for decay via either zero-temperature

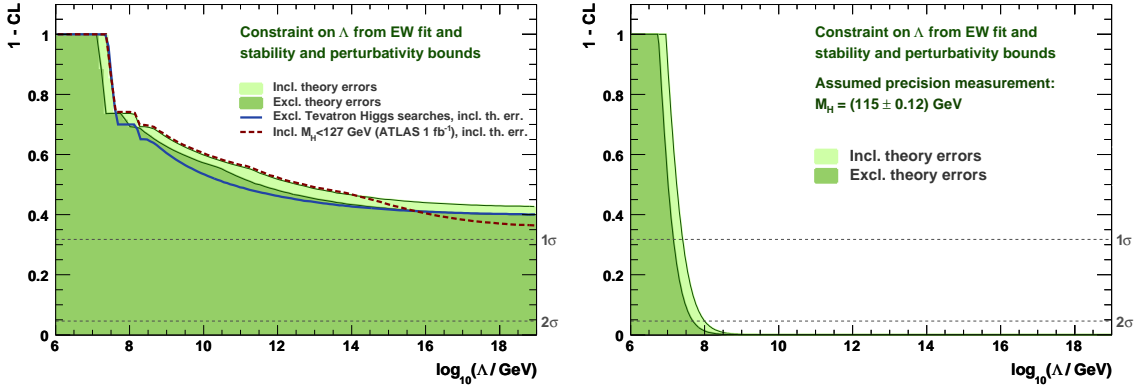


Figure 6: Left: constraint on Λ , expressed as $1 - \text{CL}$, from the global electroweak fit and the requirement of absolute vacuum stability and perturbativity. Shown are fits with (light shading) and without (dark shading) taking into account the theoretical uncertainty in the stability bound. The bold solid (blue) line shows the effect of removing the Tevatron Higgs searches from the global fit. The dashed (red) line shows the effect of a hypothetical upper bound $M_H < 127$ GeV at 95% CL, as might be obtained with early data at the LHC. Right: assuming in addition the discovery of a light Higgs with precisely measured mass of 115 GeV. Also included in the fits of this plot are improved errors for the top and W masses, as anticipated for the LHC.

quantum fluctuations (region above the dark shaded (red) band in Fig. 5) or thermal fluctuations (region above the medium shaded (blue) band). Uncertainties in these bounds stem from top-mass and α_s dependencies as well as theoretical errors mainly due to missing higher order RGE corrections. At $\Lambda = M_P$, the bounds read [27]: $M_H < (175 (173) \pm 0.8 \pm 0.1)$ GeV (nonperturbative bound for $\lambda(M_P) = 2\pi$ (π)), $M_H > (108.9 \pm 5.3 \pm 3.0)$ GeV (zero-temperature metastability), $M_H > (122.0 \pm 3.7 \pm 3.0)$ GeV (thermal metastability), and $M_H > (128.6 \pm 3.4 \pm 1.0)$ GeV (absolute vacuum stability). Between these bounds there is a range of intermediate values of M_H for which the SM could survive up to the Planck scale.

The bounds can be convolved with the M_H constraints from the global electroweak fit including the direct Higgs searches [27]. In particular the Tevatron data [18] increase the exclusion of the nonperturbative scenario from 95.7% to 99.1% CL, if $\lambda = 2\pi$ is taken to be the nonperturbative threshold. The collapse scenario is ruled out for most of the parameter region by the direct Higgs searches at LEP [17], though a small region is still compatible with the limit so that no significant exclusion CL can be set (we find a p-value of 0.40 for it being compatible with the LEP result).

Requiring absolute vacuum stability and perturbativity until $\Lambda = M_P$, and using all the available constraints on M_H , one can derive confidence levels for the maximum allowed scale Λ before new physics must come in to stabilise the Higgs potential. Figure 6 (left) shows $1 - \text{CL}$ versus Λ for various cases: with (light shaded) and without (dark shaded) the theoretical uncertainty in the stability bound, including and excluding (solid line) the results from the Tevatron Higgs boson searches, and assuming a hypothetical unsuccessful early Higgs search at one of the high- p_T LHC experiments (represented here by ATLAS), for an integrated luminosity of approximately 1 fb^{-1} at 14 TeV centre-of-mass energy, that should have sufficient sensitivity to exclude $M_H > 127$ GeV at 95% CL [28] (dashed line). No constraint on Λ that would reach or exceed 68% CL can be derived from the present data, nor from the prospective incremental improvement in the Higgs constraint

that might come from the Tevatron or the early running of the LHC. If, however, there were a Higgs discovery with a mass determined to be $M_H = 115$ GeV after years of successful LHC operation, one would obtain the constraints on Λ plotted in the right plot of Fig. 6. The 95% CL upper limits on the cut-off scale, obtained including theoretical errors, would read $\log_{10}(\Lambda/\text{GeV}) < 10.4$ and 8.0, respectively (including an almost half an order of magnitude theoretical uncertainty). In this case, one would obtain an upper limit on the absolute stability of the SM that would be comparable with the scale suggested by the seesaw model for the light neutrino masses. The p-value of the $M_H = 115$ GeV scenario for the survival of the SM up to M_P is as small as the occurrence of a 5.3σ fluctuation.

5. Concluding remarks

The efforts by many to develop with the Gfitter package a modern tool for model testing in High-Energy Physics has found its first application in a reimplementaion of the global electroweak fit leading, together with the direct Higgs boson searches, to an exclusion of Standard Model Higgs masses above 153 GeV at 95% confidence level. Exploiting new theoretical developments, the fit also provides the, as of today, theoretically most robust determination of α_s . Gfitter allows us to quantify the narrow passage for the Standard Model to survive all the way up to the Planck scale, between such catastrophic scenarios as nonperturbative blow-up or a collapsing electroweak vacuum [27]. Similar to the hierarchy problem, these scenarios manifest the instability of the Higgs field under radiative corrections.

All results presented in this review are obtained in the framework of the minimal Standard Model. Extensions of the Higgs sector [29] may evade the constraints from the electroweak precision data. The effects of these extensions on the gauge vector-boson self-energy graphs, known as oblique corrections, are known for most of the models and must be continuously confronted with the newest experimental data. Physics beyond the Standard Model should alter the high-scale behaviour of the Higgs potential, thus possibly rendering the upper bound on the Higgs mass derived from nonperturbativity irrelevant. Due to these arguments, and the strong theoretical grounds for new physics at the TeV scale, experimental Higgs searches cannot rely on the limits obtained with fits within the Standard Model, but must continue to explore all the sensitive phase space not yet excluded by direct searches.

The imminent goals for the Gfitter group are two-fold: (i) maintain the Standard Model package in line with experimental and theoretical progress, and continuously improve the Gfitter core package and the fit efficiency, (ii) extend it by plugging in new physics models. Examples for analyses beyond the Standard Model in Gfitter are the Type-II Two-Higgs-Doublet model [8,6] and oblique parameter fits [30]. The latter analysis will be diversified and, among others, augmented by Supersymmetry.

References

- [1] LEP Collaborations: ALEPH, DELPHI, L3 and OPAL (G. Alexander *et al.*), Phys. Lett. B 276, 247 (1002).
- [2] CDF Collaboration (F. Abe *et al.*), Phys. Rev. Lett. 74, 2626 (1995); D0 Collaboration (S. Abachi *et al.*), Phys. Rev. Lett. 74, 2632 (1995).

- [3] LEP Electroweak Working Group, Contributed to the 27th International Conference on High-Energy Physics – ICHEP 94, Glasgow, Scotland, UK, 20–27 Jul 1994, CERN-PPE-94-187.
- [4] D.Y. Bardin *et al.*, *Comput. Phys. Commun.* 133, 229 (2001); A.B. Arbuzov *et al.*, *Comput. Phys. Commun.* 174, 728 (2006).
- [5] G. Montagna, O. Nicosini, F. Piccinini and G. Passarino, *Comput. Phys. Commun.* 117, 278 (1999); J. Erler, *Phys. Rev. D* 63, 071301 (2001).
- [6] H. Flächer *et al.*, *Eur. Phys. J. C* 60, 543 (2009); for updated results visit the Gfitter web: <http://cern.ch/gfitter>.
- [7] R. Brun and F. Rademakers, *Nucl. Instrum. Meth. A* 389, 81 (1997).
- [8] M. Baak, these conference proceedings.
- [9] J. Espinosa, these conference proceedings.
- [10] M. Awramik, M. Czakon and A. Freitas, *JHEP* 11, 048 (2006); M. Awramik, M. Czakon, A. Freitas and G. Weiglein, *Phys. Rev. D* 69, 053006 (2004); M. Awramik, M. Czakon and A. Freitas, *Phys. Rev. Lett.* 93, 201805 (2004).
- [11] R. Boughezal and J.B. Tausk and J.J. van der Bij, *Nucl. Phys. B* 725, 3 (2005); R. Boughezal and J.B. Tausk and J.J. van der Bij, *Nucl. Phys. B* 713, 278 (2005).
- [12] Electroweak Working Group (D.Y. Bardin *et al.*), CERN-YELLOW-95-03A, hep-ph/9709229 (1997).
- [13] P.A. Baikov, K.G. Chetyrkin and J.H. Kühn, *Phys. Rev. Lett.* 101, 012002 (2008).
- [14] D0 Collaboration, Conference Note 5893-CONF (2009).
- [15] The Tevatron Electroweak Working Group, FERMILAB-TM-2439-E, arXiv:0908.1374 (Aug 2009).
- [16] Tevatron Electroweak Working Group and CDF and D0 Collaborations, CDF-NOTE-9717, D0-NOTE-5899, arXiv:0903.2503 (2009).
- [17] The ALEPH, DELPHI, L3 and OPAL Collaborations, and LEP Working Group for Higgs Boson Searches, *Phys. Lett. B* 565, 61 (2003).
- [18] Tevatron New Phenomena and Higgs Working Group for the CDF and D0 Collaborations, FERMILAB-PUB-09-060-E, arXiv:0903.4001 (2009).
- [19] CKMfitter Group (J. Charles *et al.*), *Eur. Phys. J. C* 41, 1 (2005).
- [20] M. Davier, S. Descotes-Genon, A. Höcker, B. Malaescu and Z. Zhang, *Eur. Phys. J. C* 56, 305 (2008).
- [21] M. Beneke and M. Jamin, *JHEP* 0809, 044 (2008).
- [22] S. Menke, arXiv:0904.1796 (2009).
- [23] K. Maltman and T. Yavin, *Phys. Rev. D* 78, 094020 (2008).
- [24] S. Bethke, *Prog. Part. Nucl. Phys.* 58, 351 (2007).
- [25] ATLAS Collaboration, Physics TDR, Vol. II, CERN-LHCC-99-15, 1999; CMS Collaboration, Physics TDR, Vol. II, CERN-LHCC-06-21, 2006.
- [26] A. Djouadi *et al.*, International Linear Collider Reference Design Report Volume 2: Physics at the ILC, arXiv:0709.1893 (2007).
- [27] J. Ellis *et al.*, *Phys. Lett. B* 679, 369 (2009).

- [28] ATLAS Collaboration, CERN-OPEN-2008-020, arXiv:0901.0512 (2008).
- [29] Ch. Grojean, these conference proceedings.
- [30] M. Goebel, Talk given at 44th Rencontres de Moriond EW 2009: Electroweak Interactions and Unified Theories, La Thuile, Italy, 7-14 Mar 2009, arXiv:0905.2488.